Phase-space study of the Stern-Gerlach experiment

1994 J. Phys. A: Math. Gen. 27 3511

(http://iopscience.iop.org/0305-4470/27/10/026)

J. Phys. A: Math. Gen. **27** (1994) 3511–3522. Printed in the UK

Phase-space study of the Stern–Gerlach experiment

Christian W Müller and Fritz W Metz
Fakultät für Chemie, Universität Konstanz, D-78434 Konstanz, Germany

Received 12 November 1993

Abstract. We study the motion of neutral spinning particles in static inhomogeneous magnetic fields, where the orbital motion and spin dynamic do not factorize. Using the phase-space representation of quantum mechanics, the Moyal propagator is obtained for the case of a linearized field. As an example, the evolution of particles in coherent rotational states is calculated. In order to interprete the Wigner state function in a classical mechanical way, we calculated the Husimi functions.

1. Introduction

The Wigner–Weyl–Moyal (WWM) representation of quantum mechanics has a long history [1] and attained a lot of interest. Originally formulated for spinless particles only, the extension to particles with spin $\frac{1}{2}$ was established first by means of spinor calculus [2], but this did not comply with the request for a description as closely as possible to classical ideas. It was Stratonovich [3] and much later Várilly and Gracia-Bondía [4, 5], who extended the phase-space by the unit sphere and gained a much more satisfactory phase-space representation for particles with spin $\frac{1}{2}$ and even arbitrary spin. A number of applications to particles moving in electromagnetic fields have been performed since then [6]. Allowing the interpretation of quantum mechanical states in a classical context, the WWM representation seems to be an interesting alternative to the abstract Hilbert space quantum mechanics. This applies especially for particles with spins which have no easy to grasp interpretation.

We elaborate here the case of particles moving in a static inhomogeneous magnetic field, corresponding to the Stern–Gerlach experiment [7], where the orbital motion and the spin dynamic are intertwined and cannot be factorized. We assume a beam of particles with rather well defined velocity moving perpendicular to a strong magnetic field with a strong gradient in the field direction, which are detected on a screen after leaving the field region. For atoms in a doublet state, one expects to find two well separated spots on the screen corresponding to the 'up' and 'down' components of the spin. As has been stressed in the literature (e.g. [8, 16, 17] among others), this simple picture is only a caricature of a much more complicated experimental situation. The two states have a final width and are not well separated. Particles in the state 'spin up' might be found in the spin down region and vice versa, so that there might be a real problem in assigning a pure spin state to a position on the detector screen. We expect new insight into this old problem by means of the Wigner functions which are much nearer to classical intuition than the Schrödinger function.

In order to fix notation, in the following section we give a short introduction to the WWM representation for particles with spin, which has been introduced by Várilly and Gracia-Bondía [4, 5]. In the third section, we calculate the propagator for particles with

0305-4470/94/103511+12$19.50

arbitrary spin in a linear approximated inhomogeneous magnetic field. In the fourth section, we calculate and discuss the evolution of the Wigner function of spin $\frac{1}{2}$ particles in coherent spin states by means of the Wigner state function. In order to interprete the Wigner function in a probabilistic manner, we calculate the Husimi functions from them in the last section.

2. Wigner–Weyl–Moyal quantum mechanics

For a non-relativistic particle with spin, the corresponding phase space is $\mathbb{R}^6 \otimes S^2$, which is the Kronecker product of an orbital and a spin part [5] with coordinates $\gamma \equiv (\boldsymbol{u}, \boldsymbol{n}) \equiv (\boldsymbol{q}, \boldsymbol{p}, \boldsymbol{n})$, $\boldsymbol{n} : (\theta, \phi) \mapsto (\sin\theta\cos\phi, \sin\theta\sin\phi, \cos\theta)$ representing the points of the unit sphere S^2. The non-commutative product of operators on Hilbert space translates to the so-called twisted product of the corresponding functions defined over phase space:

$$(f \times g)(\gamma) = \int_{\mathbb{R}^6 \otimes S^2} \int_{\mathbb{R}^6 \otimes S^2} f(\gamma')\, g(\gamma'')\, \mathcal{L}(\gamma, \gamma', \gamma'')\, \mathrm{d}\gamma'\, \mathrm{d}\gamma'' . \tag{1}$$

Here, f and g are functions over phase space. The measure over this space is $\mathrm{d}\gamma = \mathrm{d}\boldsymbol{u}\, \mathrm{d}\boldsymbol{n}$ with $\mathrm{d}\boldsymbol{u} = \mathrm{d}\boldsymbol{q}\, \mathrm{d}\boldsymbol{p}$, $\mathrm{d}\boldsymbol{q} = dq_x\, dq_y\, dq_z$, $\mathrm{d}\boldsymbol{p} = dp_x\, dp_y\, dp_z$ and $\mathrm{d}\boldsymbol{n} = \sin\theta\, \mathrm{d}\theta\, \mathrm{d}\phi$. $\mathcal{L}$ is the integral kernel

$$\mathcal{L}(\gamma, \gamma', \gamma'') = \exp\left[\frac{2\mathrm{i}}{\hbar}({}^t\boldsymbol{u}\boldsymbol{J}\boldsymbol{u}' + {}^t\boldsymbol{u}'\boldsymbol{J}\boldsymbol{u}'' + {}^t\boldsymbol{u}''\boldsymbol{J}\boldsymbol{u})\right]\left(\frac{2j+1}{4\pi}\right)^2 \times \sum_{r,s,t=-j}^{j} Z^j_{rs}(\boldsymbol{n}) Z^j_{st}(\boldsymbol{n}') Z^j_{tr}(\boldsymbol{n}'')$$

with ${}^t\boldsymbol{u}$ the transposed of $\boldsymbol{u}$ and the the symplectic matrix $\boldsymbol{J}$:

$$\boldsymbol{J} = \begin{pmatrix} 0 & \boldsymbol{I} \\ -\boldsymbol{I} & 0 \end{pmatrix} \tag{2}$$

$\boldsymbol{I}$ being the 3×3 identity matrix. The functions $Z^j_{rs}(\theta, \phi)$ are the Wigner functions of the transition elements $|\, jr\,\rangle\langle\, js\,|$. They are functions on the unit sphere and might be expressed [4] in terms of the usual spherical harmonics $Y_{lm}(\theta, \phi)$:

$$Z^j_{rs}(\theta, \phi) = \frac{\sqrt{4\pi}}{2j+1} \sum_{l=0}^{2j} \sqrt{2l+1} \left\langle \begin{matrix} j & l \\ r & s-r \end{matrix} \,\middle|\, \begin{matrix} j \\ s \end{matrix} \right\rangle Y_{l,s-r}(\theta, \phi) . \tag{3}$$

The evolution of an elementary particle of mass M, charge e and spin j is described by the Pauli Hamiltonian, which turns in phase-space formalism to the function

$$H(\boldsymbol{q}, \boldsymbol{p}, \boldsymbol{n}) = \frac{1}{2M}\left(\boldsymbol{p} + \frac{e}{c}\boldsymbol{A}(\boldsymbol{q})\right)^2 - \frac{e\hbar}{Mc}\boldsymbol{B}(\boldsymbol{q})\, \boldsymbol{J}(\boldsymbol{n}) + e\,\Phi(\boldsymbol{q}) \tag{4}$$

where $\boldsymbol{B} = \operatorname{rot}\boldsymbol{A}$ is the magnetic field and $\Phi(\boldsymbol{q})$ the scalar potential. The vector function $\boldsymbol{J}(\boldsymbol{n}) = \hbar\sqrt{j(j+1)}\,\boldsymbol{n}$ is associated to the vector spin operator.

The analogue of the unitary evolution operator $\hat{U} = \exp(-\mathrm{i}t\hat{H}/\hbar)$ on Hilbert space is the 'Moyal propagator'

$$\Xi(\gamma, t) = \exp_\times\left(-\frac{\mathrm{i}H(\gamma)t}{\hbar}\right) := 1 - \frac{\mathrm{i}t}{\hbar}H + \frac{1}{2!}\left(\frac{-\mathrm{i}t}{\hbar}\right)^2 H \times H + \frac{1}{3!}\left(\frac{-\mathrm{i}t}{\hbar}\right)^3 H \times H \times H + \cdots$$

with the Wigner function $H(\gamma)$ associated to $\hat{H}$.

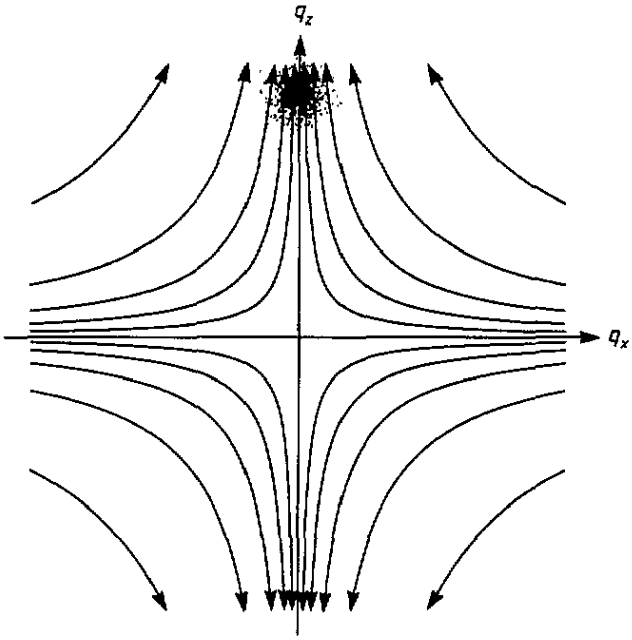

Figure 1. The magnetic field and the dotted region, where experiments typically are made. The field may be approximated in this region by a strong constant field with a small inhomogeneous correction.

3. Moyal propagator for a particle moving in an inhomogeneous static magnetic field

The Stern–Gerlach experiment has been made with electric neutral particles or atoms, which have a non-vanishing magnetic moment. We assume they are moving in an inhomogeneous magnetic field $\boldsymbol{B}(\boldsymbol{q}) = B(-q_x, 0, q_z)$, which may be derived from the vector potential $\boldsymbol{A}(\boldsymbol{q}) = B(0, q_x q_z, 0)$. Writing μ for the magnetic moment of the particle times the constant B in the magnetic field above, the relevant Hamiltonian then becomes

$$H(\boldsymbol{q}, \boldsymbol{p}, \boldsymbol{n}) = \frac{1}{2M}\boldsymbol{p}^2 - \mu\left(q_z J_z(\boldsymbol{n}) - q_x J_x(\boldsymbol{n})\right) . \tag{5}$$

In contrast to the case of any homogeneous magnetic field, spin and position operators are mixed here, and the Hamiltonian cannot be factorized into spin and orbital parts. No general analytic solution for the propagator is known for this type of problem. For special cases however, the dynamic of the particle may be calculated approximately.

We assume that experiments are taken in a field region with a relatively strong constant magnetic field, which is typical for the Stern–Gerlach experiment. This corresponds to values of q_z which are huge compared with q_x, where the effect of the $q_x J_x$ term may be neglected [8, 9].

This leads to a decoupling of the x, y and z components and the total propagator becomes a simple product of propagators for each component. Using $\boldsymbol{p} \times \boldsymbol{p} = \boldsymbol{p}^2$, we find

$$\Xi(\boldsymbol{q}, \boldsymbol{p}, \boldsymbol{n}) = \exp_\times\left(-\frac{\mathrm{i}Ht}{\hbar}\right) = \exp\left[-\frac{\mathrm{i}tp_x^2}{2M\hbar}\right] \exp\left[-\frac{\mathrm{i}tp_y^2}{2M\hbar}\right] \Xi_z(q_z, p_z, \boldsymbol{n}) \tag{6}$$

with

$$\Xi_z(q_z, p_z, \boldsymbol{n}) = \exp_\times\left[-\frac{\mathrm{i}t}{\hbar}\left(\frac{1}{2M}p_z^2 - \mu q_z J_z(\boldsymbol{n})\right)\right]. \tag{7}$$

For the x and y component, this is simply the propagator for a free particle. The Ξ_z part needs some elaboration. Since $\sum_m Z_{mm} = 1$ and expanding $J_z(\boldsymbol{n}) = \sum_m m\hbar Z_{mm}(\boldsymbol{n})$ we get

$$\Xi_z(q_z, p_z, \boldsymbol{n}) = \exp_\times\left\{\sum_{m=-j}^{j} Z_{mm}(\boldsymbol{n})\left[-\frac{\mathrm{i}t}{\hbar}\left(\frac{1}{2M}p_z^2 - m\hbar\mu q_z\right)\right]\right\}. \tag{8}$$

In view of $Z_{mm} \times Z_{m'm'} = \delta_{mm'} Z_{mm}$, we then get

$$\Xi_z(q_z, p_z, \boldsymbol{n}) = \sum_{m=-j}^{j} Z_{mm}(\boldsymbol{n}) \exp_\times\left(-\frac{\mathrm{i}t}{2M\hbar}p_z^2 + \mathrm{i}tm\mu q_z\right). \tag{9}$$

The exponential term corresponds to a quadratic Hamiltonian, for which the propagator may be calculated by means of the general formula of Gadella *et al* [10]. The propagator of a Hamilton function $H(\boldsymbol{u}) = \frac{1}{2}{}^t\boldsymbol{u}\boldsymbol{S}\boldsymbol{u} + {}^t\boldsymbol{c}\boldsymbol{u}$ with $\boldsymbol{u} = (\boldsymbol{q}, \boldsymbol{p})$, $\boldsymbol{q}, \boldsymbol{p} \in \mathbb{R}^n$ is accordingly

$$\Xi_H(\boldsymbol{u}, t) = \frac{2^n \mathrm{e}^{-\mathrm{i}b(t)/\hbar}}{\sqrt{\det(\boldsymbol{I} + \Sigma(t))}} \exp\left(\frac{\mathrm{i}}{\hbar}G(\boldsymbol{u}, t)\right) \tag{10}$$

with

$$G(\boldsymbol{u}, t) = {}^t(\boldsymbol{u} + \tfrac{1}{2}\boldsymbol{a}(t))\, \boldsymbol{J}\,(\Sigma(t) - \boldsymbol{I})\,(\Sigma(t) + \boldsymbol{I})^{-1}\, {}^t(\boldsymbol{u} + \tfrac{1}{2}\boldsymbol{a}(t))\, {}^t\boldsymbol{u}\boldsymbol{J}\boldsymbol{a}(t)$$

and

$$\boldsymbol{a}(t) = \int_0^t \Sigma(s)\boldsymbol{J}\boldsymbol{c}\,\mathrm{d}s \qquad b(t) = \tfrac{1}{2}\int_0^t \int_0^s {}^t\boldsymbol{c}\Sigma(r - s)\boldsymbol{J}\boldsymbol{c}\,\mathrm{d}r\,\mathrm{d}s$$

where $\boldsymbol{J}$ is the symplectic matrix (2) and $\Sigma(t) = \exp(-\boldsymbol{J}\boldsymbol{S}t)$. Doing some analysis we find together with (6) that

$$\Xi(\boldsymbol{u}, \boldsymbol{n}) = \sum_{m=-j}^{j} Z_{mm}(\boldsymbol{n}) \exp\left[-\frac{\mathrm{i}}{\hbar}\left(\frac{\boldsymbol{p}^2}{2M} - m\hbar\mu q_z\right)t - \frac{\mathrm{i}\hbar m^2\mu^2}{24M}t^3\right] \tag{11}$$

and for a particle with spin $j = \frac{1}{2}$

$$\Xi(\boldsymbol{u}; \theta, \phi) = \exp\left(-\frac{\mathrm{i}p^2 t}{2M\hbar} - \frac{\mathrm{i}\hbar\mu^2 t^3}{96M}\right)\left(\cos\frac{\mu q_z t}{2} + \mathrm{i}\sqrt{3}\cos\theta\sin\frac{\mu q_z t}{2}\right). \tag{12}$$

Any initial state function in phase space $\rho_0(\gamma)$ now propagates according to

$$\rho(\gamma, t) = \Xi(\gamma, t) \times \rho_0(\gamma) \times \Xi(\gamma, t)^*. \tag{13}$$

The spectral function is simply the Fourier transform of the propagator [10]

$$\Lambda_z(\gamma, E) = \frac{1}{2\pi\hbar}\int \Xi_z(\gamma, t)\mathrm{e}^{\mathrm{i}tE/\hbar}\mathrm{d}t \tag{14}$$

$$= \sum_{m=-j}^{j} Z_{mm} \sqrt[3]{\frac{8M}{m^2\mu^2\hbar^4}}\,\mathrm{Ai}\left[\sqrt[3]{\frac{8M}{m^2\mu^2\hbar^4}}\left(\frac{1}{2M}p_z^2 - m\hbar\mu q_z - E\right)\right] \tag{15}$$

with the Airy function $\mathrm{Ai}(z) = (2\pi)^{-1}\int \exp(-\mathrm{i}\nu z - \mathrm{i}\nu^3/3)\,\mathrm{d}\nu$.

4. Evolution of a coherent spin state

Let us first look at coherent rotational states (CRS) in the WWM formalism. The CRS [12] are the eigenstates of the operator $\boldsymbol{a}\hat{\boldsymbol{J}}$, with eigenvalue $\hbar j$ and orientation vector $\boldsymbol{a} \in \mathbb{R}^3$, $|\boldsymbol{a}| = 1$. Let the corresponding Wigner function be denoted by $\zeta_{\boldsymbol{a}}$. This function is most easily obtained from the spectral function of $\boldsymbol{a}\hat{\boldsymbol{J}}$. Let $\boldsymbol{R}(\boldsymbol{a}) \in SO(3)$ be a rotation operator, which turns the 'north' pole $(0, 0, 1)$ to $\boldsymbol{a}$ and $\hat{J}_z$ to $\boldsymbol{a}\hat{\boldsymbol{J}}$. The phase-space function $J_z(\boldsymbol{n})$ is transformed into $J_{\boldsymbol{a}}(\boldsymbol{n}) = \sum_m m\hbar Z^j_{mm}(\boldsymbol{R}(\boldsymbol{a})\boldsymbol{n})$ with the associated propagator

$$\Xi_{\boldsymbol{a}}(\boldsymbol{n}, t) = \exp\left(-\frac{\mathrm{i}}{\hbar} J_{\boldsymbol{a}}(\boldsymbol{n})t\right) = \sum_{m=-j}^{j} \mathrm{e}^{-\mathrm{i}mt} Z^j_{mm}(\boldsymbol{R}(\boldsymbol{a})\boldsymbol{n})\,. \tag{16}$$

The spectral function

$$\Lambda_{\boldsymbol{a}}(\boldsymbol{n}, E) = \frac{1}{2\pi\hbar}\int \Xi_{\boldsymbol{a}}(\boldsymbol{n}, t)\mathrm{e}^{\mathrm{i}tE/\hbar}\,\mathrm{d}t = \sum_{m=-j}^{j} \delta(E - m\hbar) Z^j_{mm}(\boldsymbol{R}(\boldsymbol{a})\boldsymbol{n}) \tag{17}$$

yields at $E = \hbar j$ the eigenfunction $\zeta_{\boldsymbol{a}} = Z^j_{jj}(\boldsymbol{R}(\boldsymbol{a})\boldsymbol{n})$. For a spin-$\frac{1}{2}$ particle in a pure state $|\alpha, \beta\rangle$ with $|\alpha|^2 + |\beta|^2 = 1$, this function may be written as

$$\zeta_{\boldsymbol{a}}(\boldsymbol{n}) = \frac{1}{2} + \frac{\sqrt{3}}{2}\boldsymbol{a}\boldsymbol{n} \tag{18}$$

with $\boldsymbol{a} = (Re\, 2\alpha^*\beta, Im\, 2\alpha^*\beta, \alpha^*\alpha - \beta^*\beta)$.

Let the initial wavepacket, which enters the magnetic field region, be a product of some function $\phi(\boldsymbol{q})$ in configuration space and a pure spin function. We restrict our consideration to minimum uncertainty wavepackets, whose geometric centre about $\langle\hat{\boldsymbol{q}}\rangle = \boldsymbol{q}_0$ and $\langle\hat{\boldsymbol{p}}\rangle = \boldsymbol{p}_0 = M\boldsymbol{v}$ moves with velocity $\boldsymbol{v}$

$$\phi(\boldsymbol{q}) = \frac{1}{(\delta\sqrt{\pi})^{3/2}} \exp\left[-\frac{(\boldsymbol{q} - \boldsymbol{q}_0)^2}{2\delta^2}\right] \exp\left[\frac{\mathrm{i}}{\hbar}\boldsymbol{p}_0\boldsymbol{q}\right]. \tag{19}$$

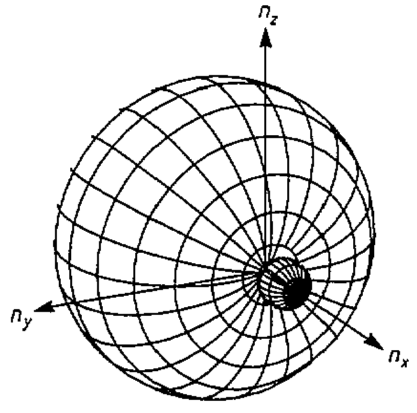

Figure 2. The spin part of the initial Wigner function, which is a coherent rotational state, polarized in the x-direction. It is shown from behind in order to display the negative part, which is the smaller ball.

Units are choosen such that $\delta = 1$ and $\hbar = 1$. We apply the parity operator [11] on (19) and get the corresponding Wigner function:

$$\rho(q, p, n) = \frac{1}{\pi^3} \int_{\mathbb{R}^3} e^{-2ips} \phi^*(q - s)\phi(q + s)\, ds \tag{20}$$
$$= \frac{1}{\pi^3} \exp\left[(q - q_0)^2\right] \exp\left[-(p - p_0)^2\right] .$$

The total phase-space function is the product of the coherent spin state function (18) and the orbital part (20):

$$\rho_a(q, p, n) = \frac{1}{\pi^3} \exp\left[-(q - q_0)^2\right] \exp\left[-(p - p_0)^2\right] \left(\frac{1}{2} + \frac{\sqrt{3}}{2} an\right) . \tag{21}$$

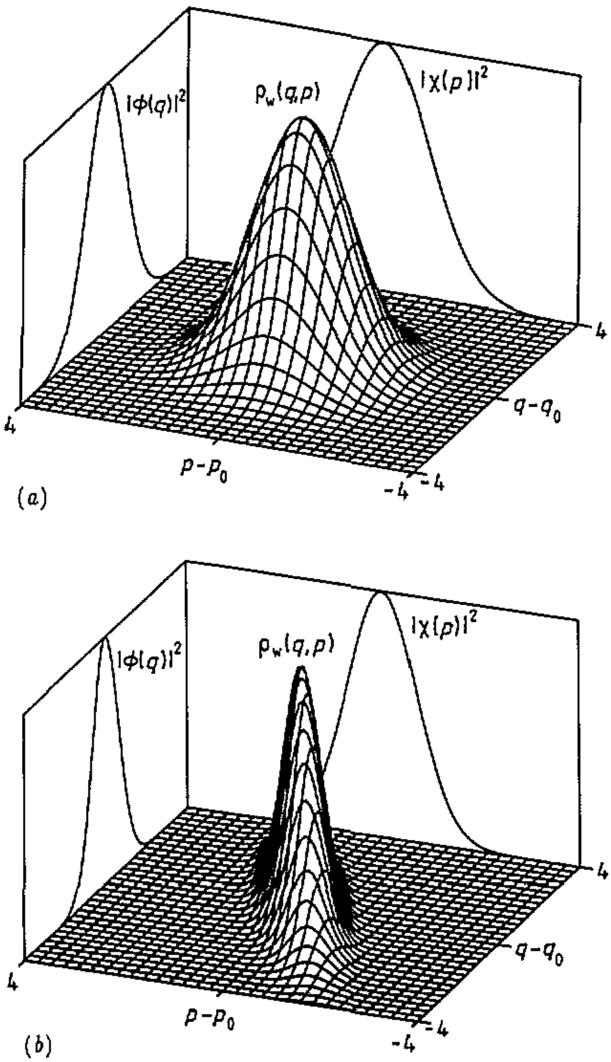

Figure 3. Free evolution of the minimum uncertainty Wigner function (23) for $t = 0$ (a) and $t = \frac{3}{2}$ (b). The configuration probability density (33) is projected onto the left-hand side and the momentum probability density (34) is projected onto behind in arbitrary units.

The time evolution of this state function may be calculated according to (13) and (1) and we get

$$\rho_a(\boldsymbol{q}, \boldsymbol{p}, \boldsymbol{n}, t) = \rho^{(x)}(q_x, p_x, t)\, \rho^{(y)}(q_y, p_y, t)\, \rho_a^{(z)}(q_z, p_z, \boldsymbol{n}, t) \tag{22}$$

with

$$\rho^{(x)}(q, p, t) = \rho^{(y)}(q, p, t) = \frac{1}{\pi} \exp\left[-(q - q_0 - pt/M)^2\right] \exp\left[-(p - p_0)^2\right] \tag{23}$$

and

$$\begin{aligned}
\rho_a^{(z)}(q, p, \theta, \phi, t) \\
= \frac{1}{\pi} \Bigg\{ & \frac{1 + a_z}{2} \exp\left[-(q - q_0 - pt/M + \mu t^2/4M)^2\right] \\
& \times \exp\left[-(p - p_0 - \mu t/2)^2\right] \left(\frac{1}{2} + \frac{\sqrt{3}}{2} \cos\theta\right) \\
& + \frac{1 - a_z}{2} \exp\left[-(q - q_0 - pt/M - \mu t^2/4M)^2\right] \\
& \times \exp\left[-(p - p_0 + \mu t/2)^2\right] \left(\frac{1}{2} - \frac{\sqrt{3}}{2} \cos\theta\right) \\
& + \exp\left[-(q - q_0 - pt/M)^2\right] \\
& \times \exp\left[-(p - p_0)^2\right] \frac{\sqrt{3}}{2} \sin\theta \Big(a_x \cos\varphi + a_y \sin\varphi\Big) \Bigg\}
\end{aligned} \tag{24}$$

with $\varphi = \phi - \mu t(q - pt/2M)$.

Parts of this function are plotted for different times in figures 3, 4 and 5 together with the corresponding probability densities in momentum and configuration space obtained by integration as explained in the appendix. Figure 3 shows the orbital part of the spin averaged Wigner function. For the y-direction, where the magnetic field is homogeneous, this is especially the free evolution of the wavepacket. Note that the Wigner function of the wavepacket undergoes merely a deformation in phase space which has a natural explanation in terms of classical mechanics. This has to be contrasted with the evolution of the probability density in configuration space, where due to neglecting the momentum information only a spread is observed. This type of broadening which results from the rotation of the wavepacket in orbital phase space described by a complex width parameter should be carefully distinguished from the irreversible spreading due to diffusion processes, which must be described by real width parameters.

Similarly, as shown in figure 4, where the evolution parallel to the static component of the magnetic field is shown, we find a much stronger effect in phase space than in configuration or momentum space. Almost complete separation of the spin 'up' and spin 'down' component of the spin averaged wavefunction is found in figure 4(b) at time $t = \frac{5}{2}$, where there is none in configuration space and still a strong overlap in momentum space.

That the spin part of the Wigner function also carries some interesting information is seen in figure 5. The spin part is shown here at the lower maximum of the orbital part for the times $t = \frac{3}{2}$ and $t = \frac{5}{2}$. It has to be compared with the spin function at $t = 0$ from figure 2. At $t = \frac{5}{2}$ the spin function has almost reached its final value with the direction of the maximum parallel to the $-\boldsymbol{e}_z$ axis and a shape, that is typical for a pure spin state like the one shown in figure 2.

The direction of the maximum of the spin part moved from an angle of 90° to the $-\boldsymbol{e}_z$ axis at $t = 0$ to about 38° at $t = \frac{3}{2}$, however the shape shows, that this is neither a pure nor

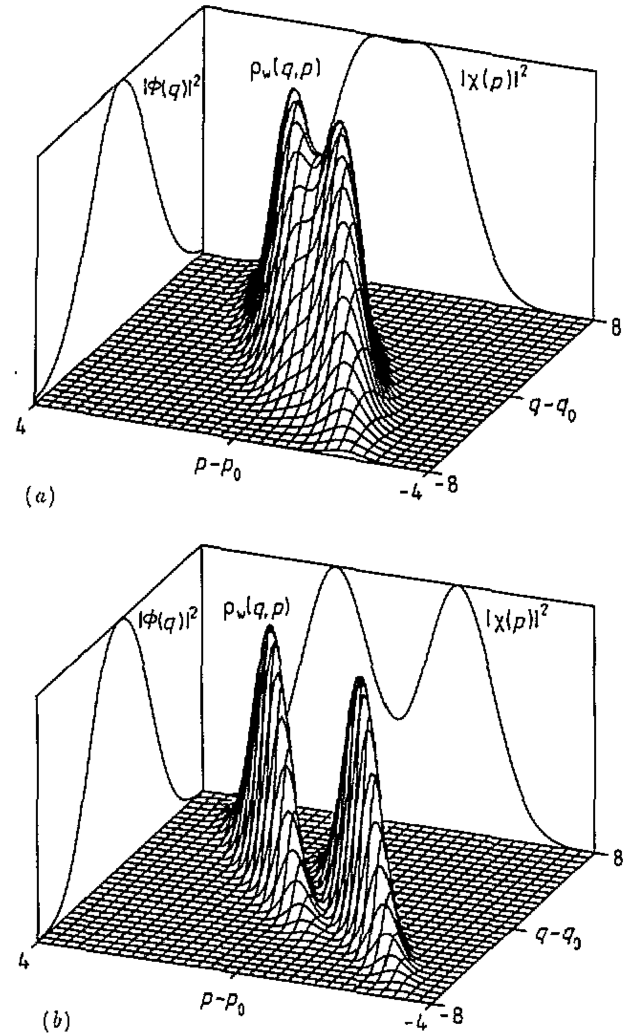

Figure 4. The propagated minimum uncertainty Wigner function (24) after integration over all spin directions, and projected onto the z-direction, where the magnetic field is inhomogeneous for time $t = \frac{3}{2}$ (a) and $t = \frac{5}{2}$ (b). We have choosen $q_0 = 10$. The configuration and momentum probability density is projected as in figure 3.

a conventional mixed spin state with positive eigenvalues. Because of the intertwinement of the spin and orbital motion in this region, there is no simple interpretation [15], similar to the negative probabilities of Wigner functions on the orbital phase space.

5. Probabilities in phase space

In order to interprete the Wigner phase-space function in a classical mechanical way, we need some kind of smoothing procedure, that washes out the pseudoprobability structure. Most famous is the family of Husimi functions ρ_σ^{H} [13, 14], which is essentially the expectation value of the density operator $\hat{\rho}$ in some squeezed coherent state $|q/\sigma, \sigma p\rangle$ of the Weyl

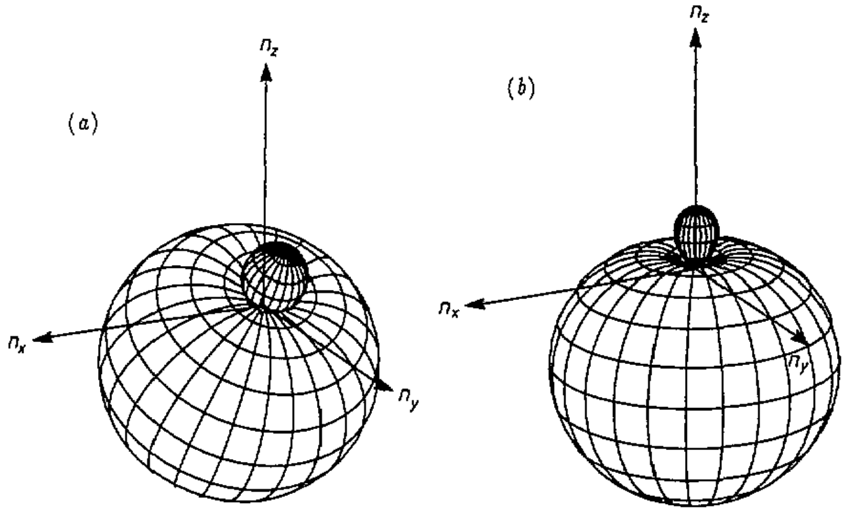

Figure 5. Spin part of the propagated Wigner function (24) at time $t = \frac{3}{2}$, $(q, p) = (9.5, -0.75)$ (a) and $t = \frac{5}{2}$, $(q, p) = (8.5, -1.25)$ (*b*), where the orbital part of the Wigner function reaches a maximum (see figure 3).

algebra with the squeezing parameter σ

$$\rho_\sigma^{\mathrm{H}}(\boldsymbol{q}, \boldsymbol{p}) = \langle \boldsymbol{q}/\sigma, \sigma \boldsymbol{p} | \hat{\rho} | \boldsymbol{q}/\sigma, \sigma \boldsymbol{p} \rangle . \tag{25}$$

It has a simple probabilistic interpretation and in the limiting cases $\sigma \to 0$ and $\sigma \to \infty$ we recover the configuration resp. momentum probability density

$$\lim_{\sigma \to 0} \rho_\sigma^{\mathrm{H}}(\boldsymbol{q}, \boldsymbol{p})/\sigma = |\phi(\boldsymbol{q})|^2 \tag{26}$$

$$\lim_{\sigma \to \infty} \rho_\sigma^{\mathrm{H}}(\boldsymbol{q}, \boldsymbol{p})\sigma = |\chi(\boldsymbol{p})|^2 . \tag{27}$$

In a similar way we may define the Husimi analogue function $Q_{\boldsymbol{a}}$ of the CRS $|\boldsymbol{a}\rangle$ as

$$Q_{\boldsymbol{a}}(\boldsymbol{n}) = \langle \boldsymbol{n} | \boldsymbol{a} \rangle \langle \boldsymbol{a} | \boldsymbol{n} \rangle = \int_{S^2} \zeta_{\boldsymbol{n}}(\boldsymbol{n}') \zeta_{\boldsymbol{a}}(\boldsymbol{n}') \, \mathrm{d}\boldsymbol{n}' = \tfrac{1}{2} + \tfrac{1}{2} \boldsymbol{a}\boldsymbol{n} . \tag{28}$$

The Husimi function may be calculated directly from the Wigner function ρ^{W} by convolution with the Wigner function of the squeezed coherent state $|\boldsymbol{q}/\sigma, \sigma \boldsymbol{p}\rangle$

$$\rho_\sigma^{\mathrm{H}}(\boldsymbol{q}, \boldsymbol{p}) = \frac{1}{\pi} \int_{\mathbb{R}^6} \rho^{\mathrm{W}}(\boldsymbol{q}', \boldsymbol{p}') \mathrm{e}^{-(\boldsymbol{q}'-\boldsymbol{q})^2/\sigma^2 - (\boldsymbol{p}'-\boldsymbol{p})^2 \sigma^2} \, \mathrm{d}\boldsymbol{q}' \, \mathrm{d}\boldsymbol{p}' . \tag{29}$$

Integrating over all spin directions, we obtain from (24) the Husimi function ρ_σ^{H} (again only for the z-direction)

$$\begin{aligned} \rho_\sigma^{\mathrm{H}}(q, p) &= \frac{1 - a_z}{2} \rho_{\sigma,-1/2}^{\mathrm{H}} + \frac{1 + a_z}{2} \rho_{\sigma,1/2}^{\mathrm{H}} \\ &= \sqrt{\frac{\sigma^2}{(1+\sigma^2)^2 + (t/M)^2}} \exp\left[-\frac{\sigma^2}{1+\sigma^2} (p - p_0 - \mu m t)^2 \right] \\ &\quad \times \exp\left\{ -\left[q - q_0 + \mu m t^2 (\sigma^2 - 1)/(1+\sigma^2) 2M \right.\right. \\ &\quad \left.\left. -(\sigma^2 p + p_0) t/(1+\sigma^2) M \right]^2 \big/ \left[1 + \sigma^2 + (t/M)^2/(1+\sigma^2) \right] \right\} . \end{aligned} \tag{30}$$

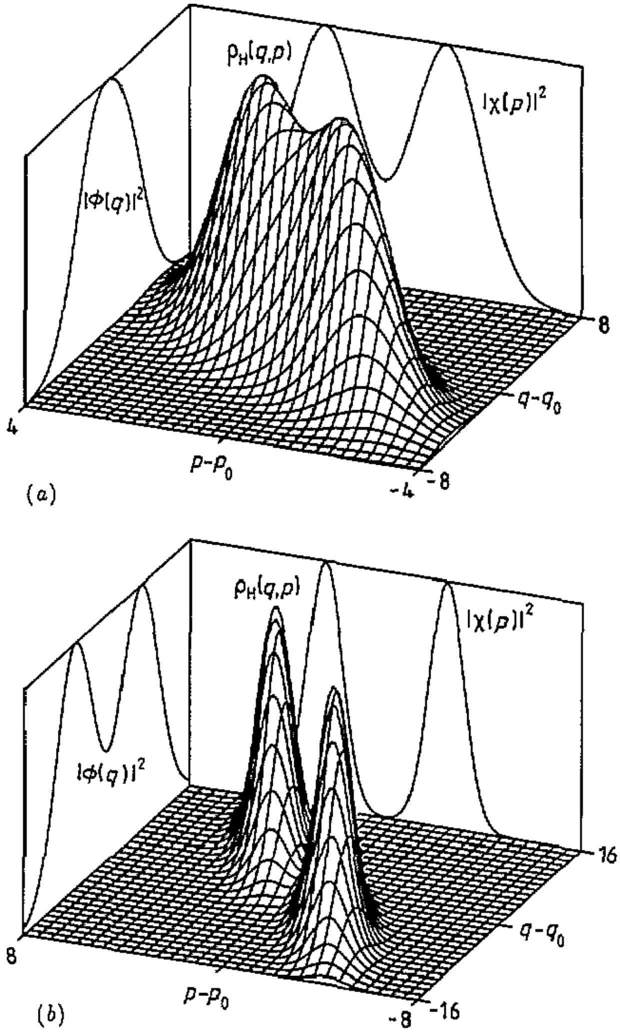

Figure 6. The Husimi function (30) after integration over all spin directions at time $t = \frac{5}{2}$ (*a*) and $t = 5$ (*b*). The configuration and momentum probability density (26) and (27) is also shown as in figure 3.

For a qualitative comparison we give a surface plot of the two phase space distributions (24) and (30) in figure 7. The parabola is the classical trajectory, which corresponds in accordance with the Ehrenfest theorem to the position and momentum expectation values, thus the centre of the Gaussian state functions. We remark that in addition to the shear flow discussed above, we now observe also in phase space an additional spread increasing *with a time-dependent factor* $[1 + (t/4M)^2]^{1/2}$ *similar to the one found in the configuration* space density. This is the price one has to pay for a probabilistic interpretation on the basis of the CS of the Weyl algebra. However this factor might be partially reduced by choosing a squeezing parameter $\sigma > 1$ or a correlated squeezed state with the largest axis parallel to the average velocity of the Husimi function. The latter are most easily obtained by a free evolution of the unified state along a second path which avoids the region of the

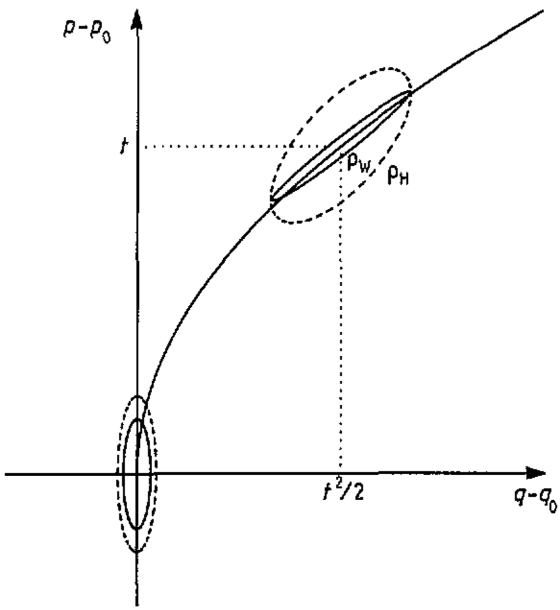

Figure 7. Surface plot of the Wigner function ρ^W (24) (full curve) and the Husimi function ρ_σ^H (30) with $\sigma = 1$ (broken curve) at time $t = 5$ for the spin 'up' component. We have plotted here only the uncertainty ellipses, where the function values are half their maximum value. The parabola corresponds to the classical trajectory.

magnetic field and combines somewhere with one of the Stern–Gerlach components similar to standard double slit experiments.

6. Summary

We show that the Wigner–Weyl–Moyal formalism provides an interesting approach to the time evolution of spinning particles in inhomogeneous magnetic fields. For large times, one finds two well separated regions of particles in pure spin 'up' resp. 'down' state. The time-dependent spreading, which is well known from the evolution of wavepackets in configuration space, does not occure for the Wigner function. For intermediate times however, there is a intertwinement of spin and orbital motion, so that there is no simple interpretation of the spin state or orbital parts of the Wigner function. Husimi functions do not suffer from this drawback, but they reintroduce the undesired spreading if they are based on coherent states with their axes fixed in phase space.

Acknowledgment

FWM gratefully acknowledges financial support by the 'Fonds der Chemischen Industrie'.

Appendix

The configuration or momentum probability density, as shown in figures 3, 4 and 6 is found by integration of the Wigner function

$$|\phi(q)|^2 = \int_{\mathbb{R}^3\times S^2} \rho^{\mathrm{W}}(q,p,n)\,\mathrm{d}p\,\mathrm{d}n \tag{31}$$

$$|\chi(p)|^2 = \int_{\mathbb{R}^3\times S^2} \rho^{\mathrm{W}}(q,p,n)\,\mathrm{d}q\,\mathrm{d}n \tag{32}$$

where the configuration representation is connected with the momentum representation via the Fourier transform

$$\chi(p) = \frac{1}{(2\pi)^3}\int_{\mathbb{R}^3} \mathrm{e}^{-\mathrm{i}qp}\phi(q)\,\mathrm{d}q\,.$$

We obtain from (24), again only for the z coordinates

$$\begin{aligned}|\phi(q)|^2 = \sqrt{\frac{1+(t/M)^2}{\pi}}\Bigg\{&(1+a_z)\exp\left[-\frac{[q-q_0+\mu t^2/4M-(p_0+\mu t/2)t/M]^2}{1+(t/M)^2}\right]\\ &+(1-a_z)\exp\left[-\frac{[q-q_0-\mu t^2/4M-(p_0-\mu t/2)t/M]^2}{1+(t/M)^2}\right]\Bigg\}\end{aligned} \tag{33}$$

and

$$\begin{aligned}|\chi(p)|^2 = \sqrt{\frac{1}{\pi}}\,\big\{&(1+a_z)\exp\left[-(p-p_0-\mu t/2)^2\right]\\ &+(1-a_z)\exp\left[-(p-p_0+\mu t/2)^2\right]\big\}\,.\end{aligned} \tag{34}$$

References

[1] Wigner E P 1932 *Phys. Rev.* **40** 749
Weyl H 1928 *Gruppentheorie und Quantenmechanik* (Leipzig: Hirzel)
Moyal J E 1949 *Proc. Camb. Phil. Soc.* **45** 99
[2] Carruthers P and Zachariasen F 1983 *Rev. Mod. Phys.* **55** 245
O'Connell 1984 *Phys. Rev.* A **30** 2613
[3] Stratonovich R L 1957 *Sov. Phys.–JETP* **4** 891
[4] Várilly J C and Gracia-Bondía J M 1989 *Ann. Phys.* **190** 107
[5] Gracia-Bondía J M and Várilly J C 1988 *J. Phys. A: Math. Gen.* **21** L879
[6] Nieto L M 1991 *J. Phys. A: Math. Gen.* **24** 1579; 1992 *J. Math. Phys.* **33** 3402
Fernandez C D J and Nieto L M 1991 *Phys. Lett.* **157** 315; 1991 *Phys. Lett.* **161** 202
[7] Stern O 1921 *Z. Phys.* **7** 249
Gerlach W and Stern O 1921 *Z. Phys.* **8** 110; 1922 *Z. Phys.* **9** 349, 352
[8] Scully M O, Lamb W E and Barut A 1987 *Found. Phys.* **17** 575
[9] Aerts D and Reignier J 1989 *VUB/TENA/89/08*
[10] Gadella M, Gracia-Bondía J M, Nieto L M and Várilly J C 1989 *J. Phys. A: Math. Gen.* **22** 2709
[11] Grossmann A 1976 *Commun. Math. Phys.* **48** 191
Royer A 1977 *Phys. Rev.* A **15** 449
[12] Arrecchi F T, Courtens E, Gilmore R and Thomas H 1972 *Phys. Rev.* D **6** 2211
[13] Husimi K 1940 *Proc. Phys. Math. Soc. Japan* **22** 264
[14] Hillery M, O'Connell R F, Scully M O and Wigner E P 1984 *Phys. Rep.* **106** 121
[15] Müller C W 1994 in preparation
[16] Garbaczewski P 1988 *Problems in quantum physics (Gdańsk '87)* ed L Kostro, A Posiewnik, J Pykacz and M Zukowski (Singapore: World Scientific) p 494
[17] Martens H and de Muynck W M 1993 *J. Phys. A: Math. Gen.* **26** 2001